New Phytologist

Research

The leaf polarity factors SGS3 and YABBYs regulate style elongation through auxin signaling in *Mimulus lewisii*

Baoqing Ding[1,5]*, Jingjian Li[1,2]*, Vandana Gurung[1], Qiaoshan Lin[1], Xuemei Sun[3] and Yao-Wu Yuan[1,4]

[1]Department of Ecology and Evolutionary Biology, University of Connecticut, Storrs, CT 06269, USA; [2]College of Forestry and Landscape Architecture, South China Agricultural University, Guangzhou 510642, China; [3]Qinghai Key Laboratory of Genetics and Physiology of Vegetables, Qinghai University, Xining 810008, China; [4]Institute for Systems Genomics, University of Connecticut, Storrs, CT 06269, USA; [5]Current address: College of Horticulture, Nanjing Agricultural University, Nanjing 210095, China

Authors for correspondence:
Baoqing Ding
Email: ding.baoqing@gmail.com

Yao-Wu Yuan
Email: yuan.colreeze@gmail.com

Received: *23 June 2021*
Accepted: *18 August 2021*

New Phytologist (2021) **232:** 2191–2206
doi: 10.1111/nph.17702

Key words: auxin signaling, monkeyflowers (*Mimulus*), pistil, SGS3, style elongation, YABBY.

Summary

- Style length is a major determinant of breeding strategies in flowering plants and can vary dramatically between and within species. However, little is known about the genetic and developmental control of style elongation.
- We characterized the role of two classes of leaf adaxial–abaxial polarity factors, SUPPRESSOR OF GENE SILENCING3 (SGS3) and the YABBY family transcription factors, in the regulation of style elongation in *Mimulus lewisii*. We also examined the spatiotemporal patterns of auxin response during style development.
- Loss of *SGS3* function led to reduced style length via limiting cell division, and downregulation of *YABBY* genes by RNA interference resulted in shorter styles by decreasing both cell division and cell elongation. We discovered an auxin response minimum between the stigma and ovary during the early stages of pistil development that marks style differentiation. Subsequent redistribution of auxin response to this region was correlated with style elongation. Auxin response was substantially altered when both *SGS3* and *YABBY* functions were disrupted.
- We suggest that auxin signaling plays a central role in style elongation and that the way in which auxin signaling controls the different cell division and elongation patterns underpinning natural style length variation is a major question for future research.

Introduction

Most flowering plants bear both male and female reproductive organs in each of their flowers (Renner, 2014). The relative positions of the two sexual organs in different species determine their reproductive strategies and ensure pollination precision and efficiency (Barrett *et al.*, 2000; Barrett, 2019). For example, species that are predominantly outcrossing usually bear flowers with stigma well above anther to avoid self-pollination. However, stigma and anther are generally located at similar heights in selfing species. For most flowers, the height of the female organ (i.e. pistil) is largely determined by the style length, which can vary dramatically not only between species (Goodwillie *et al.*, 2006; Wessinger *et al.*, 2014; Fishman *et al.*, 2015; Hermann *et al.*, 2015; Kostyun *et al.*, 2019), but also within many species (Ganders, 1979; Dulberger, 1992; Huu *et al.*, 2016; Arunkumar *et al.*, 2017). In fact, Darwin devoted much of his book *The Different Forms of Flowers on Plants of the Same Species* (Darwin, 1877) to a particular type of intraspecific style length variation – heterostyly, where the different floral forms of the same species produce either long styles and short stamens, or short styles and long stamens. Despite the long-lasting interest in style length variation (Darwin, 1877; Barrett, 2002, 2010), the genetic and developmental control of style elongation remains poorly understood.

Numerous genetic mapping experiments have been carried out to identify the loci underlying style length variation between species in multiple plant lineages, including *Mimulus* (Bradshaw *et al.*, 1995; Fishman *et al.*, 2002, 2015), *Solanum* (Bernacchi & Tanksley, 1997; Georgiady *et al.*, 2002; Chen & Tanksley, 2004; Chen *et al.*, 2007), *Leptosiphon* (Goodwillie *et al.*, 2006), *Penstemon* (Wessinger *et al.*, 2014), *Petunia* (Hermann *et al.*, 2015) and *Jaltomata* (Kostyun *et al.*, 2019). However, only one of these studies has identified the actual causal gene: the reduced style length in a domesticated tomato cultivar compared with wild tomatoes was caused by a regulatory mutation in a gene (*STYLE2.1*) encoding a basic helix–loop–helix (bHLH) protein (Chen *et al.*, 2007). More recently, two promising MYB transcription factors have been implicated in controlling style length variation between closely related *Petunia* species (Yarahmadov *et al.*, 2020), but their causality remains to be further tested. Likewise, extensive effort has been made to pinpoint the genes responsible for heterostyly within species (Labonne & Shore,

*These authors contributed equally to this work.

2011; Ushijima *et al.*, 2015; Huu *et al.*, 2016; Yasui *et al.*, 2016; Arunkumar *et al.*, 2017). However, so far, only a *CYP734A50* gene, encoding a putative brassinosteroid-degrading enzyme, has been experimentally demonstrated to determine the style length dimorphism in heterostylous *Primula* species (Huu *et al.*, 2016).

Through mutant analyses in the genetic model system Arabidopsis (*Arabidopsis thaliana*), several transcriptional regulators required for proper style development have been identified. These include the auxin response factor ETTIN (ARF3) (Sessions *et al.*, 1997; Simonini *et al.*, 2016), the zinc finger proteins STYLISH1 and STYLISH2 (Kuusk *et al.*, 2002), the bHLH proteins SPATULA and INDEHISCENT (Heisler *et al.*, 2001; Liljegren *et al.*, 2004; Moubayidin & Østergaard, 2014), the homeodomain-containing proteins REPLUMLESS and BREVIPEDICELLUS (Venglat *et al.*, 2002; Roeder *et al.*, 2003), and the molecular adaptor protein SEUSS (Franks *et al.*, 2002; Pfluger & Zambryski, 2004). It has been proposed that ETTIN/ARF3, through a noncanonical auxin-sensing mechanism (Simonini *et al.*, 2016), functions as an auxin gradient interpreter (Nemhauser *et al.*, 2000) and interacts with INDEHISCENT, REPLUMLESS, BREVIPEDICELLUS, and SEUSS to direct style morphogenesis (Simonini *et al.*, 2018). However, essentially all these transcriptional regulators are involved in tissue specification (i.e. differentiation of the style tissue from the ovary and stigma), not style elongation *per se*. The extremely short style of Arabidopsis compared with the vast majority of flowering plant species (Simonini & Østergaard, 2019) makes it challenging to separate style specification and elongation as two distinct developmental processes. Indeed, none of these Arabidopsis genes has been implicated in the aforementioned genetic analyses of style length variation in natural species. Thus, it is currently unclear whether these Arabidopsis style specification genes also regulate style elongation, and, if so, how they relate to the few style elongation genes uncovered in other species (Chen *et al.*, 2007; Huu *et al.*, 2016; Yarahmadov *et al.*, 2020). It is also unclear whether the structure of the genetic network controlling style elongation will allow us to predict 'hotspot' genes that are preferentially selected by evolution (Stern, 2011) to generate style length variation in nature.

The ideal plant systems to address these questions should have the following features: producing flowers with elongated styles; being amenable to rigorous genetic and developmental analyses; and displaying a great deal of natural variation in style length. One system with all these features is the monkeyflower *Mimulus lewisii* species complex, which contains several closely related species with remarkable style length variation (Bradshaw *et al.*, 1995; Fishman *et al.*, 2015) and is amenable to routine chemical mutagenesis and transgenic manipulation (Yuan *et al.*, 2013a, 2014; Sagawa *et al.*, 2016; Ding *et al.*, 2017, 2020; Stanley *et al.*, 2020). The wild-type *M. lewisii* (inbred line LF10) flower contains two pairs of stamens, one pair slightly longer than the other, and a syncarpous pistil with two fused carpels, an elongated style and two stigma lobes (Fig. 1a).

Here we show that two classes of leaf adaxial–abaxial polarity regulators, SUPPRESSOR OF GENE SILENCING3 (SGS3) and the YABBY family transcription factors, promote style elongation in *M. lewisii*. In Arabidopsis, SGS3 is part of the *trans*-acting small interfering RNA (tasiRNA) biogenesis pathway that produces the tasiARF small RNAs in the adaxial side of leaf primordium and restricts the expression of their target genes *ARF3* and *ARF4* to the abaxial side (Garcia *et al.*, 2006; Hunter *et al.*, 2006; Chitwood *et al.*, 2009). Together with the adaxial-localized ASYMMETRIC LEAVES1 and 2 (AS1-AS2) complex and the class III homeodomain-leucine zipper (HD-ZIPIII) transcription factors, the SGS3-tasiARF module helps to determine the adaxial identity of leaf primordium. Similarly, the abaxial-localized ARF3/4, KANADI and YABBY transcription factors determine abaxial cell fate (Nakata & Okada, 2013; Tsukaya, 2013; Kuhlemeier & Timmermans, 2016). This spatial separation of the expression domain of adaxial and abaxial determinants is largely attributed to their mutually antagonistic interactions (Wu *et al.*, 2008; Iwasaki *et al.*, 2013; Merelo *et al.*, 2013; Huang *et al.*, 2014). Furthermore, many of these adaxial–abaxial polarity determinants were shown to directly regulate genes involved in auxin biosynthesis, transport and signaling (Brandt *et al.*, 2012; Merelo *et al.*, 2013; Huang *et al.*, 2014; Simonini *et al.*, 2016), which is critical to coordinate leaf laminar growth at the adaxial–abaxial boundary (Waites & Hudson, 1995; Kuhlemeier &

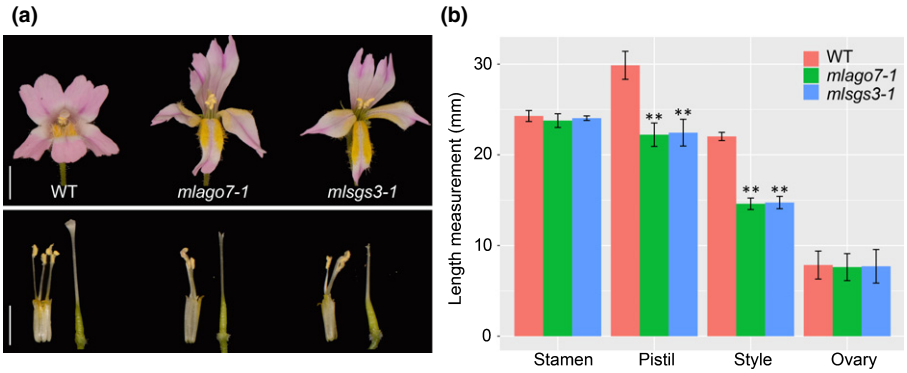

Fig. 1 Phenotypic characterization of the reproductive organs for the *Mimulus lewisii* wild-type (LF10) and the *ago7* and *sgs3* mutants. (a) Front view of the flowers (above) and side view of the stamens and pistil (below). Bars, 10 mm. (b) Length measurements of the long stamen, pistil, style and ovary of fully open flowers. Error bars represent 1 SD from 10 flowers for each genotype. Asterisks indicate differences from the wild-type (**, $P < 0.01$, Student's *t*-test).

Timmermans, 2016). Therefore, we hypothesized that *SGS3* and the *YABBY* genes may regulate style elongation in *M. lewisii* through modulating auxin dynamics.

Using the DR5 auxin-responsive promoter, we discovered an auxin response minimum between the stigma lobes and the ovary during early stages of pistil development in the wild-type *M. lewisii*, which marks the region that differentiates into the style. Subsequent redistribution of auxin response to this region was correlated with style elongation. When both SGS3 and YABBY functions were disrupted, style length was severely reduced and auxin response patterns were also substantially altered. We suggest that the spatiotemporal dynamics of auxin signaling in the developing pistil might be a key to understanding the genetic and developmental regulation of style elongation.

Materials and Methods

Plant materials and growth conditions

The *Mimulus lewisii* inbred line LF10 (wild-type) and the *sgs3* mutant (*mlsgs3-1*) have been described previously (Yuan *et al.*, 2013b; Ding *et al.*, 2020). All plants were grown in the University of Connecticut research glasshouses under natural light supplemented with sodium vapor lamps, ensuring a 16 h day length with a light intensity of 110–160 μmol m^{-2} s^{-1}.

Sequence retrieval and phylogenetic analysis

The Arabidopsis YABBY transcription factors FILAMENTOUS FLOWER (FIL, AT2G45190) and CRABS CLAW (CRC, AT1G69180) were used as queries to retrieve the *M. lewisii YABBY* genes from the LF10 genome v.2.0 by tBLASTN searches at http://new-cizin.cyverse.org/ (Han *et al.*, 2009). Seven genes were found to encode proteins that are 166–233 amino acids long and contain both a C_2C_2 zinc finger domain and a helix–loop–helix 'YABBY' domain, which are defining features of the YABBY family transcription factors (Bowman, 2000). Multiple sequence alignment (Supporting Information Fig. S1) of YABBY proteins from Arabidopsis, snapdragon (*Antirrhinum majus*) and *M. lewisii* were performed in ALIVIEW (Larsson, 2014). The conserved zinc finger and YABBY domains were included in subsequent phylogenetic analysis. Parsimony analysis was conducted using PAUP* v.4.0a168 (Swofford, 2002). Heuristic searches were performed with 200 random stepwise addition replicates and Tree-Bisection-Reconnection (TBR) branch swapping with MULTREES option effective. Clade support was determined by bootstrap analyses of 200 replicates.

Plasmid construction and plant transformation

To knock down the expression of *MlYAB1*, *MlYAB2*, *MlYAB3* and *MlYAB5* simultaneously, we built an RNA interference (RNAi) construct by cloning a mosaic DNA fragment into the pFGC5941 vector (ABRC stock no. CD3-447; Kerschen *et al.*, 2004) in both sense and antisense directions, following Yuan *et al.* (2013b). This mosaic DNA fragment was produced by connecting *c.* 180–320 bp exonic sequences from each of the four genes through overlap extension PCR. BLASTING this mosaic DNA fragment against the LF10 genome did not match any regions other than the four *YABBY* genes, indicating target specificity. The final plasmid was verified by sequencing before being transformed into *Agrobacterium tumefaciens* GV3101 for subsequent plant transformation following procedures described in Yuan *et al.* (2013b). Primers used for plasmid construction are listed in Table S1.

Phenotypic characterization

We measured the lengths of the long stamen (from the base of the corolla tube to the tip of the anther) and the pistil as well as its composite ovary and style of open flowers from the wild-type and various mutant and transgenic lines with a digital caliper. For the *MlYAB* RNAi lines, we also measured petal lobe length and width, corolla tube length and calyx length. To examine the cellular basis of style length difference between the wild-type and the mutant and transgenic lines, we profiled both cell number and cell length along the entire length of the style. To do so, freshly excised styles were kept in water between a cover glass and a microscope slide. A series of overlapping images along the entire style were acquired using a Zeiss Axioskop microscope connected to a QImaging MicroPublisher 3.3 RTV camera (QImaging, Surrey, BC, Canada). ZEISS ZEN 2.6 LITE (blue edition) software was used to assemble the images into a single panoramic image (examples were shown in Fig. S2), which was then used to count the cell number and calculate cell length with the Multi-Measure Plugin in IMAGEJ (Abramoff *et al.*, 2004). All data for phenotypic quantification were analyzed in R (R Development Core Team, 2021).

Scanning electron microscopy

Flower buds were fixed overnight in formalin-acetic-alcohol (FAA) at 4°C, dehydrated for 30 min through a 50%, 60%, 70%, 95% and 100% (v/v) alcohol series. Samples were then critical point-dried, mounted and sputter-coated before being observed using a NOVA NanoSEM with Oxford EDX at 35 kV in the Bioscience Electron Microscopy Laboratory at the University of Connecticut.

Fluorescence imaging

DR5rev:mRFPer reporter lines were imaged using a Nikon A1R confocal laser scanning microscope with a ×10 objective and the excitation wavelength of 558 nm. As the length of styles exceeds the field of view under the ×10, a multipoint tile scan was used to acquire multipoint Z-stack montages. Briefly, the Z-stack was first defined in the 'ND Acquisition', with the XY tab selected. The number of tiles in the scan area was then defined in the 'Large Image' tab. The final images were derived from the superposition of a series of confocal optical sections along the *Z* axis.

NPA treatments

For N-1-naphthylphthalamic acid (NPA) treatments, lateral shoot apices of well-branched wild-type plants, including all flower buds

smaller than 5 mm on each lateral shoot, were sprayed with 100 μM NPA (Fisher Scientific, Waltham, MA, USA) as described in Nemhauser *et al.* (2000), with slight modifications. N-1-naphthylphthalamic acid was dissolved in dimethyl sulfoxide (DMSO) to a stock concentration of 100 mM. Plants were sprayed with a heavy mist of 100 μM NPA with 0.1% (v/v) Silwet L-77, and then placed in a vacuum chamber with a pressure of 28 in Hg for 2 min before being released quickly. Mock treatments were performed with distilled water containing 0.1% (v/v) Silwet L-77 and 0.1% (v/v) DMSO. After vacuum infiltration, plants were placed in moisture tents for 24 h, followed by a heavy spray with distilled water to rinse off the treatment, before being returned to regular glasshouse conditions.

Expression analyses by RT-qPCR

Total RNA was isolated using the Spectrum Plant Total RNA Kit (Sigma-Aldrich, St Louis, MO, USA) and then treated with amplification grade DNaseI (Invitrogen, Waltham, MA, USA). cDNA was synthesized from 1 μg of the DNase-treated RNA using the SuperScript III First-Strand Synthesis System (Invitrogen), then diluted 10-fold before quantitative reverse transcription polymerase chain reaction (RT-qPCR). The *M. lewisii* ortholog of Arabidopsis ubiquitin-conjugating enzyme gene (At5g25760), *MlUBC*, was used as a reference gene as described in Yuan *et al.* (2013b). Quantitative RT-PCR was performed using iQ SYBR Green Supermix (Bio-Rad, Hercules, CA, USA) in a CFX96 Touch Real-Time PCR Detection System (Bio-Rad). Samples were amplified for 40 cycles of 95°C for 15 s and 60°C for 30 s. Reactions were run with three biological replicates. Amplification efficiencies for each primer pair were determined using critical threshold values obtained from a dilution series (1 : 4, 1 : 8, 1 : 16, 1 : 32). Gene-specific primers used for RT-qPCR are listed in Table S1.

Accession numbers

Sequence data from this article can be found in GenBank or the Arabidopsis Information Resource (TAIR) database under the following accession numbers: MlYAB1, MW023905; MlYAB2, MW023907; MlYAB3, MW023904; MlYAB5, MW023906; MlINO, MW023910; MlCRC1, MW023908; MlCRC2, MW023909; AmGRAM, AY451396; AmPROL, AY451397; AmYAB2, AY451398; AmINO, AY451400; AmCRC, AY451399; AtFIL, AT2G45190; AtYAB2, AT1G08465; AtYAB3, AT4G00180; AtYAB5, AT2G26580; AtINO, AT1G23420; AtCRC, AT1G69180; MlAS1, MW424415; MlKAN1a, MW424416; MlKAN1b, MW424417; MlKAN2, MW424418.

Results

MlSGS3 regulates style elongation in *Mimulus* through cell division

Previously, we observed that loss-of-function mutations in *FLAYED1* (*MlAGO7*) and *FLAYED2* (*MlSGS3*), two genes in the tasiRNA-*ARF* pathway, caused split corolla tubes and reduced style length in *M. lewisii* (Ding *et al.*, 2020). While corolla tube formation was the focus of the previous study, the style length phenotype was not characterized in detail. To quantify the style phenotypes, here we measured the lengths of the pistil as well as its composite ovary and style for the wild-type LF10, *flayed1* (*mlago7-1*) and *flayed2* (*mlsgs3-1*). We also measured the lengths of the long stamen as control. We found that the pistils are *c.* 7.5 mm shorter in the mutants compared with the wild-type, but stamen length remains unchanged (Fig. 1b; Table S2). Furthermore, the difference in pistil length is entirely attributed to style length, as ovary length is the same between the wild-type and the mutants. Because *MlAGO7* and *MlSGS3* function in the same tasiRNA biogenesis pathway (where *SGS3* is downstream of *AGO7*) that fine-tunes the expression levels of *MlARF3* and *MlARF4*, and the loss-of-function mutants *mlago7-1* and *mlsgs3-1* are morphologically indistinguishable (Ding *et al.*, 2020; Fig. 1), we chose to focus on *mlsgs3-1* for the rest of this study.

To determine whether the reduction of the style length in *mlsgs3-1* is caused by decreased cell number or cell length, styles of fully opened flowers from the wild-type and the mutant were excised at the junction between the ovary and the style. We then profiled both cell number and cell size along the entire length of the excised style (Figs 2, S2). In the wild-type style, cell length gradually increases from the base (i.e. ovary-style junction), plateaus between the 60th and 170th cells, then gradually decreases to the top (i.e. style–stigma junction) (Fig. 2a; Table S3). The cells in the middle plateau zone are much more elongated than the cells at the base, and the cells at the top region are broadly lobed on the margin (Fig. 2b). The *mlsgs3-1* mutant has similar cell length along the style as the wild-type (Fig. 2a), but has a significantly smaller number of cells (*mlsgs3-1*, 153.33 ± 13.50 vs wild-type, 214.33 ± 6.66; $n = 3$, $P < 0.01$), indicating that the reduction of cell number is responsible for the shorter style in the mutant. Notably, the cells at the top region of the *mlsgs3-1* style are similar to the middle region in length and morphology (without lobes on the margin), as if the *mlsgs3-1* style completely lacks the counterpart top region of the wild-type.

The YABBY family transcription factors regulate style length in *Mimulus* through both cell division and cell elongation

SGS3 and AGO7 are well-known adaxial regulators required for the generation of tasiRNAs to help establish proper leaf adaxial/abaxial polarity and enable leaf laminar growth (Allen *et al.*, 2005; Axtell *et al.*, 2006; Fahlgren *et al.*, 2006; Garcia *et al.*, 2006; Hunter *et al.*, 2006; Nagasaki *et al.*, 2007; Nogueira *et al.*, 2007; Douglas *et al.*, 2010; Yan *et al.*, 2010; Yifhar *et al.*, 2012; Zhou *et al.*, 2013). This prompted us to ask whether the regulatory role in style elongation is peculiar to the adaxial factors such as the AGO7-SGS3-tasiRNA module, or abaxial components of the leaf polarity network are also involved in style length regulation. To address this question, we chose to study the YABBY family transcription factors for two reasons. First, in Arabidopsis, *YAB1/FIL*, *YAB2*, *YAB3* and *YAB5* function redundantly

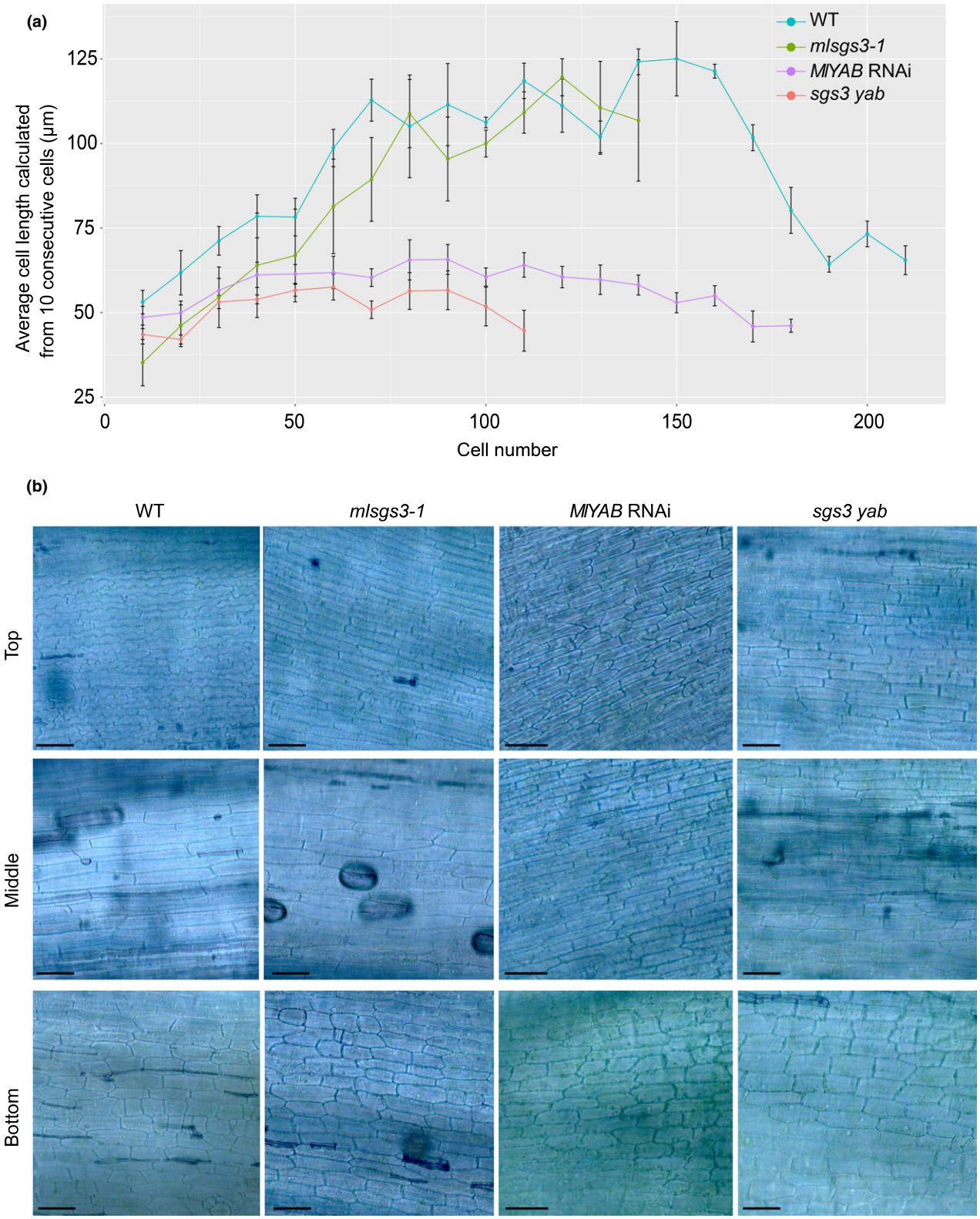

Fig. 2 Characterization of the cellular differences between the wild-type and various genetic lines. (a) Cell profiling from the base (style–ovary junction) to the top (style–stigma junction) of the style of fully open flowers. The number of cells and the average cell length across the style are shown on the *x*- and *y*-axes, respectively. Error bars represent 1 SE from three biological replicates for each genotype. (b) Representative images from the base, middle ('plateau zone') and top of the style, showing cell morphology. Bars, 50 μm.

to promote abaxial cell fate and laminar growth during leaf development (Eshed *et al.*, 1999; Sawa *et al.*, 1999; Villanueva *et al.*, 1999; Bowman, 2000; Golz *et al.*, 2004). Quadruple *yab* mutants show altered auxin patterning (Sarojam *et al.*, 2010), and auxin has long been proposed as a morphogen to specify regional tissue identities during pistil development in Arabidopsis (Nemhauser *et al.*, 2000). Second, loss-of-function mutations in the *YABBY* genes cause less severe deformation in the genocium than mutations in the *KANADI* genes, the other main abaxial determinant (Golz *et al.*, 2004; Pekker *et al.*, 2005; Sarojam *et al.*, 2010). We thus expected that functional perturbation of *YABBY* genes is likely to generate specific phenotypes (e.g. style length) without causing overly severe malformation of the entire pistil.

To examine if the *YABBY* genes regulate style elongation in *Mimulus*, we first isolated the *YABBY* homologs from the *M. lewisii* LF10 genome. There are seven *YABBY* family genes in *M. lewisii* (Fig. 3a), encoding proteins that are 166–233 amino acids long with both a C_2C_2 zinc finger domain and a helix–loop–helix 'YABBY' domain (Bowman, 2000). Four of them (i.e. *MlYAB1/2/3/5*) fall into the same clade as Arabidopsis *YAB1/2/3/5*, two of them are closely related to *AtCRC*, and the other one is orthologous to *AtINO* (*AtYAB4*) (Fig. 3a). We then examined the expression patterns of *MlYAB1*, *MlYAB2*, *MlYAB3* and *MlYAB5* across multiple dissected floral organs derived from two different developmental stages by RT-PCR, and found that they all are expressed in multiple floral organs (Fig. 3b). Notably, all four *YABBY* genes are expressed at higher levels in the style/pistil than in the stamens, suggesting that these four homologs may function redundantly in pistil development. To test this possibility, we knocked down the expression of all four genes simultaneously by RNAi. To this end, we constructed an RNAi plasmid with the inverted repeat consisting of a *c.* 180–320 bp fragment from each of the four genes, and transformed the wild-type LF10 with this construct. We obtained 92 stable transgenic lines (referred to as *MlYAB* RNAi lines hereafter) with a range of phenotypes. Over two-thirds of the RNAi lines showed slower growth compared with the wild-type and narrower and shorter leaf blade with a smaller leaf-to-stem angle (i.e. more erect) (Fig. S3a,b). The length and width of the petal lobes of some *MlYAB* RNAi lines are slightly different from the wild-type, but no clear trend was observed. The corolla tube of the strongest *MlYAB* RNAi lines is slightly shorter than the wild-type, and the calyx length is moderately but consistently shorter in the *MlYAB* RNAi lines (Figs 3c, S3c). Most notably, these transgenic lines display a strong reduction in pistil length and a moderate reduction in stamen length (Fig. 3c,d). To verify that these *YABBY* genes are indeed knocked down by RNAi, we performed RT-qPCR and found that the transcript abundances of all four genes are reduced by more than 90% in a representative, strong *MlYAB* RNAi line (line 64) (Fig. 3e).

To determine whether the change of style length in the *MlYAB* RNAi lines is a result of reduction in cell number or cell size, we profiled cell number and size along the entire length of the excised style of *MlYAB* RNAi line. We found a significant reduction in both cell number (*MlYAB* RNAi, 184.33 ± 6.66 vs wild-type, 214.33 ± 6.66; $n = 3$, $P < 0.01$) and cell length (Fig. 2; Table S3) in the *MlYAB* RNAi line, indicating that these *YABBY* genes regulate both cell division and cell elongation in the *M. lewisii* style.

MlSGS3 and *MlYABs* act synergistically in style elongation

To test whether *MlSGS3* and *MlYABs* genetically interact in the regulation of style length, we crossed the *MlYAB* RNAi (line 64) transgene into the *mlsgs3-1* mutant background (referred to as the *sgs3 yab* line hereafter). The *sgs3 yab* line showed even slower growth, narrower, and shorter leaf blade than the *mlsgs3-1* single mutant or *MlYAB* RNAi lines (Fig. S4). The overall flower morphology of *sgs3 yab* is similar to *mlsgs3-1* (Fig. 4a), but some flowers have a deeper split between the two dorsal petals than *mlsgs3-1*. In occasional flowers, the two lateral petals are much less expanded and form a hollow, cylindrical structure (Fig. 4b; also see Fig. 5f), indicating malfunction of the petal adaxial–abaxial identity program. Style length of *sgs3 yab* shows severe reduction. Compared with the wild-type, style length is reduced by 33%, 44% and 68% in *mlsgs3-1*, *MlYAB* RNAi line 64 and the *sgs3 yab* line, respectively (Fig. 4c; Table S2). This suggests that *MlSGS3* and *MlYABs* function synergistically in the regulation of style length. This is further corroborated by profiling the cell number and length of the *sgs3 yab* styles, which are both substantially reduced (Fig. 2a). However, it should be noted that the first 50 cells from the base are similar in length among the different genotypes. Cell length only starts to diverge from the sixth 10-cell block and onwards (Fig. 2b). This suggests that the bottom region of the style may be regulated independently from the rest of the style. It is also worth noting that the loss/reduction of *MlSGS3* and *MlYABs* function did not show a synergistic effect in stamen or ovary length; the *sgs3 yab* line is similar to *MlYAB* RNAi in stamen and ovary length.

To further test whether *MlSGS3* and *MlYABs* regulates the expression of each other, we performed RT-qPCR of *MlSGS3* and the four *MlYAB* genes on the dissected style and ovary from 15 mm flower buds, a stage where floral organs, including the style, are in an exponential growth phase (Hazle, 2001). We found that in both the style and ovary, the *MlYAB* genes have similar expression levels between wild-type and *mlsgs3-1* (Fig. 4d, e). Likewise, *MlSGS3* expression level is not altered in the *MlYAB* RNAi background. These results suggest that *MlSGS3* and *MlYAB* do not regulate the expression of each other; instead, they may function in parallel, converging to regulate style development through some shared downstream target genes. *MlARF3* and *MlARF4* are obvious candidates for the downstream targets as they were known to be moderately upregulated in *mlsgs3-1* whole floral buds (Ding *et al.*, 2020), although whether there is a regulatory relationship between *MlYABs* and *MlARF3/4* was unknown.

To test whether *MlARF3* and *MlARF4* show synergistic upregulation in the *sgs3 yab* line, we compared the expression levels of these two genes in the dissected style and ovary of the wild-type, *mlsgs3-1*, *MlYAB* RNAi and *sgs3 yab* plants. Indeed, we found that *MlARF3* and *MlARF4* upregulation is more substantial in the style of *sgs3 yab* than in either *mlsgs3-1* or *MlYAB* RNAi

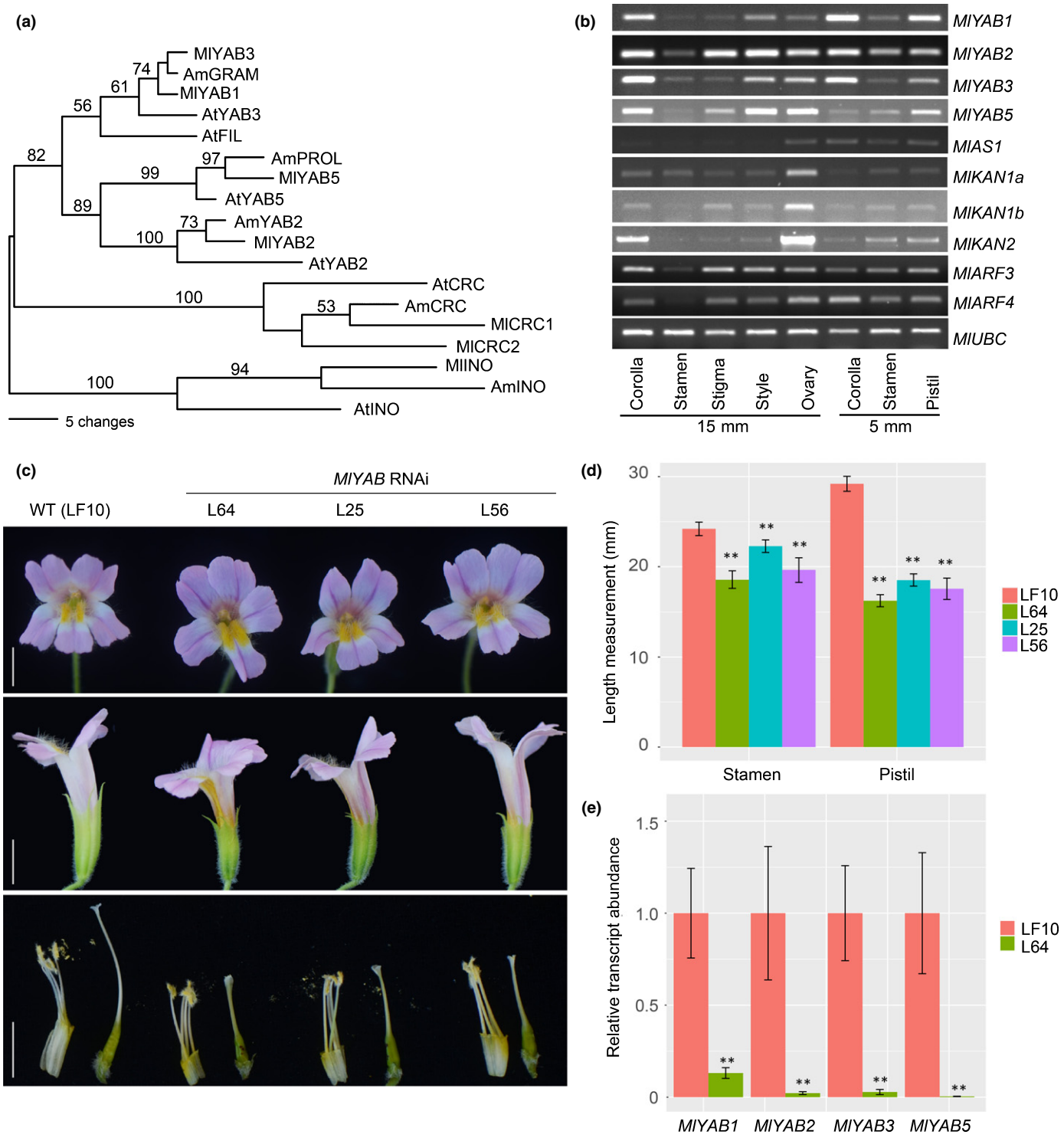

Fig. 3 Transgenic characterization of the *MIYAB* genes. (a) One of six most parsimonious trees depicting phylogenetic relationships of the YABBY family transcription factors from Arabidopsis, snapdragon (*Antirrhinum majus*) and *Mimulus lewisii*. (b) Reverse transcription polymerase chain reaction (28 cycles) of *MIYAB1/2/3/5* and other adaxial–abaxial polarity regulators in different floral organs dissected from 5 mm and 15 mm floral buds. (c) Floral phenotypes of three *MIYAB* RNA interference (RNAi) lines compared with the wild-type. Bars, 10 mm. (d) Stamen and pistil lengths of three *MIYAB* RNAi lines compared with the wild-type (WT). Error bars represent 1 SD from 12 open flowers for each line. (e) Relative transcript abundances of *MIYAB1/2/3/5* in 15 mm floral buds of *MIYAB* RNAi line 64 compared with the wild-type, as estimated by quantitative reverse transcription polymerase chain reaction. *MIUBC* was used as the reference gene. Error bars represent 1 SD from three biological replicates. Asterisks indicate differences from the wild-type (**, $P < 0.01$, Student's *t*-test).

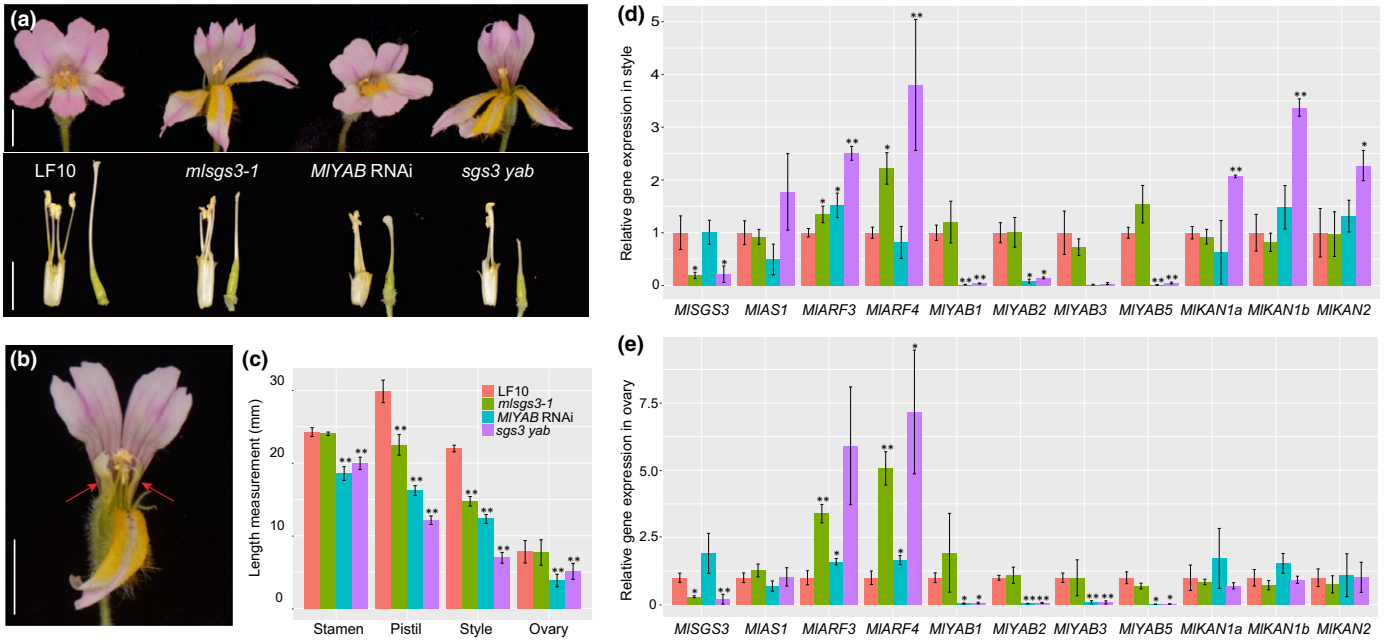

Fig. 4 Characterization of the *sgs3 yab* line. (a) Front view of the flowers (above) and side view of the stamens and pistil (below). (b) Some flowers on the *sgs3 yab* plants have lateral petals (red arrows) that are much less expanded and rod-like. Bars, 10 mm. (c) Length measurements of the stamen, pistil, style and ovary. Note that the data for the wild-type LF10 and *mlsgs3-1* are the same as shown in Fig. 1(b), but re-plotted here for comparisons. Error bars represent 1 SD from 10 flowers for each genotype. (d, e) Relative transcript abundances of *MlYAB1/2/3/5*, *MlSGS3* and other adaxial–abaxial polarity regulators in 15 mm floral bud styles (d) and ovaries (e), as estimated by quantitative reverse transcription polymerase chain reaction. *MlUBC* was used as the reference gene. Error bars represent 1 SD from three biological replicates. Asterisks indicate differences from the wild-type (*, $P < 0.05$; **, $P < 0.01$; Student's *t*-test).

(Fig. 4d), correlating with the more severe style phenotype of the *sgs3 yab* line. Somewhat surprisingly, we observed the same trend of *MlARF3/4* upregulation in the ovary (Fig. 4e), which did not show a more severe phenotype in *sgs3 yab*. We also assayed gene expression levels of the three homologs of the abaxial factor *KANADI* (*MlKAN1a*, *MlKAN1b* and *MlKAN2*), as KANADI has been shown to physically interact with ARF3 in Arabidopsis to regulate leaf polarity (Kelley *et al.*, 2012). We found that all three *KANADI* homologs are expressed significantly more highly in *sgs3 yab* than in *mlsgs3-1* or *MlYAB* RNAi, but only in the style (Fig. 4d,e), indicating that the style and ovary may be regulated by different developmental programs from that in Arabidopsis (Nemhauser *et al.*, 2000). By contrast, the adaxial factor *MlAS1* showed no significant upregulation in any of the genotypes compared with the wild-type. Taken together, these results suggest that *MlSGS3* and *MlYABs* may act synergistically in style elongation through the ARF3-KANADI regulatory complex.

The *sgs3 yab* line lacks clear boundaries among stigma, style and ovary

To further understand how style length is affected in *sgs3 yab*, we compared pistil development between the wild-type and the *sgs3 yab* line using scanning electronic microscopy. The developmental stages of wild-type *M. lewisii* flowers have been described based on the size of the corolla (Ding *et al.*, 2020). In the very early stages when floral organ primordia just initiate, the width (diameter) of the corolla is larger than the height. The pistil primordium starts to initiate at the center of the floral apex when the corolla is 0.2 mm in diameter, differentiates rapidly to form a rim at the apex when the corolla is 0.3 mm wide, and is separated into two locules by a transverse septum when the corolla is 0.4 mm (Ding *et al.*, 2020). The two stigma lobes are clearly differentiated when the corolla reaches 1.0 mm, a stage when the corolla becomes globular (Fig. 5a) and starts to grow much faster in length than width (the developmental stages will be described by the length of the corolla after the 1.0 mm stage). The style then initiates as a region of attenuation between the stigma lobes and the ovary and begins to elongate (Fig. 5b,c). This entire process of *M. lewisii* pistil organogenesis is very similar to that of the closely related species *M. cardinalis* (Hazle & Canne-Hilliker, 2005). In *sgs3 yab*, the two carpels are not completely fused towards the apex of the pistil, and the stigmas are not differentiated into the flared lobes as in the wild-type. Furthermore, there is no 'attenuation zone' between the stigma and the ovary (i.e. no clear boundary between the stigma and style or between the style and the ovary) (Fig. 5d–f). These observations suggest that both specification and elongation of the style are hampered in *sgs3 yab*.

The dynamics of auxin signaling is altered in *sgs3 yab*

It has been suggested that auxin signaling plays a vital role in Arabidopsis pistil development as well as the regional tissue specification in the gynoecium (Nemhauser *et al.*, 2000). Considering that both *SGS3* and *YABBY* genes are known to be involved in

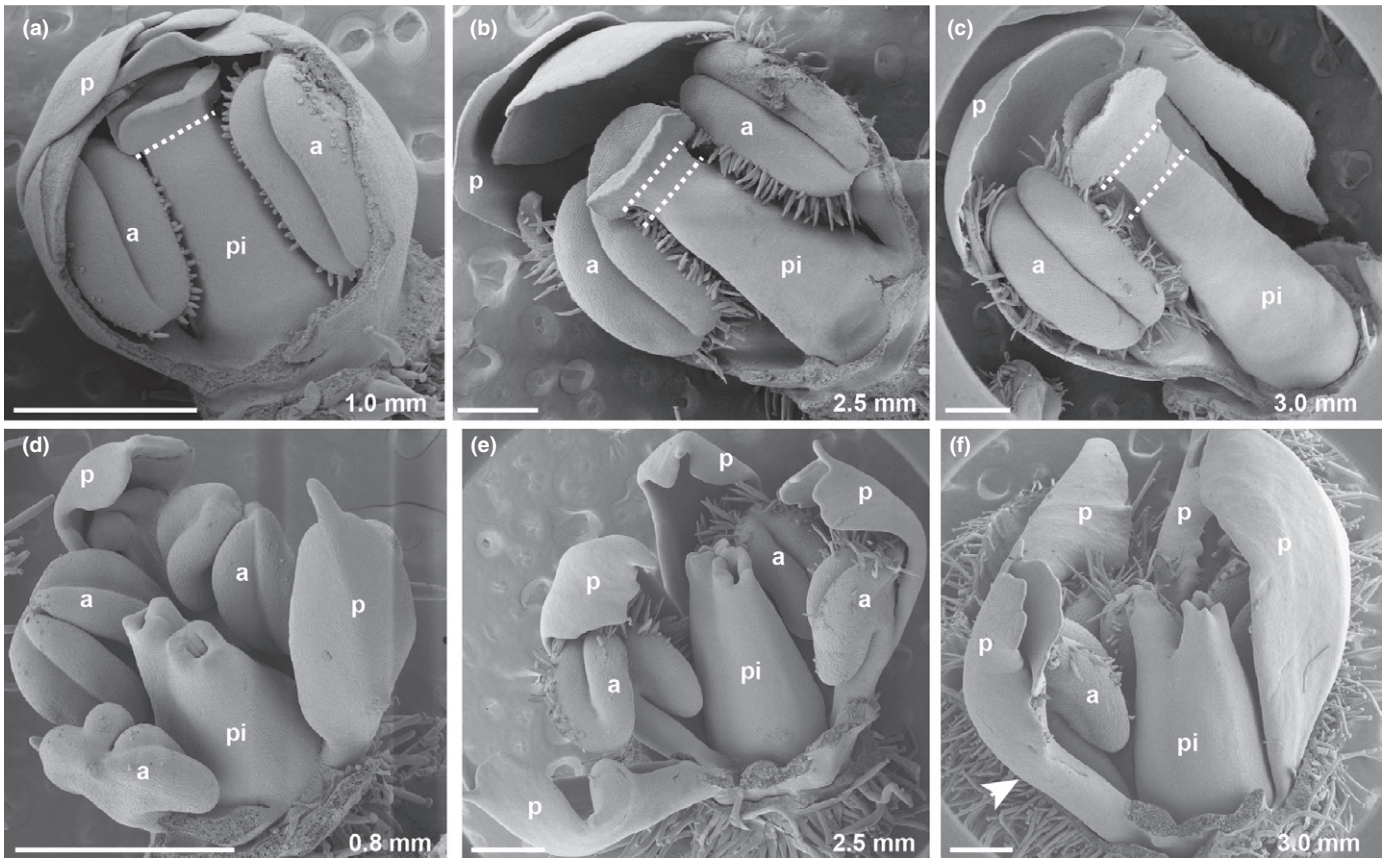

Fig. 5 Scanning electron micrographs of pistil development in wild-type *Mimulus lewisii* (a–c) and the *sgs3 yab* line (d–f). The developmental stages are marked by the length of the corolla on the bottom right of each image. The dashed lines in (a–c) mark the boundary between the stigma and style or between the style and the ovary. The white arrowhead in (f) points to the lateral petalthat is radialized and rod-like. a, anther; p, petal; pi, pistil. Bars, 500 μm.

the patterning of auxin response (Sarojam *et al.*, 2010; Ding *et al.*, 2020), we speculated that auxin signaling may have been substantially altered in the pistil of the *sgs3 yab* line. To test this hypothesis, we introduced the auxin-responsive reporter *DR5rev:mRFPer* into the *mlsgs3-1*, *MlYAB* RNAi, and the *sgs3 yab* backgrounds by crossing a previously generated *DR5rev:mRFPer* reporter line in the wild-type LF10 (Ding *et al.*, 2020) with each mutant or/and RNAi genotype. When the entire style excised from the 15 mm or equivalent floral bud stage was examined for the DR5 signal, we did not find a drastic change in the *MlYAB* RNAi background (Fig. 6a,b). By contrast, the *mlsgs3-1* mutant showed high auxin response only along a few parallel veins (instead of one central vein as in the wild-type), and very little signal between the veins or at the apex of the style. The *sgs3 yab* line showed a similar pattern to *mlsgs3-1*, almost completely lacking DR5 signals between the parallel veins or at the style apex. The lack of DR5 signal at the style apex correlates with the malformation of the stigma lobes in *mlsgs3-1* and the *sgs3 yab* line.

To examine the dynamics of auxin response through style development, we sampled pistils at four additional developmental stages before the 15 mm stage. Interestingly, in the wild-type we observed an auxin response minimum zone right below the stigma lobes at the 2 mm (corolla length) stage (Fig. 6c), corresponding to the attenuation zone where the style is differentiated from the stigma and the ovary (Fig. 5b,c). This auxin minimum is maintained for some time until auxin appears to be redistributed to this zone after the 5 mm stage. This redistribution of auxin signaling correlates with the elongation of the style (Fig. 6c). A similar auxin response pattern was observed in the *MlYAB* RNAi background across developmental stages, although the DR5 signal was generally weaker than in the wild-type when imaged under the same microscopy parameters (Fig. 6e). The difference in DR5 signal intensity is particularly obvious in the ovary (compare Fig. 6c and 6e), providing a potential explanation to the shorter ovary of *MlYAB* RNAi (Fig. 4c). There were clear differences between the *mlsgs3-1* mutant and the wild-type from the 5 mm stage onwards in that the two stigma lobes were not properly formed and the DR5 signal was restricted to the few parallel veins in the style (Fig. 6d). However, the auxin response pattern in the ovary is similar between *mlsgs3-1* and the wild-type, consistent with ovary length (Fig. 4c). The *sgs3 yab* line showed a synergistic effect, with weaker DR5 signal in the ovary and vein-restricted DR5 signal in the short style region compared with the wild-type (Fig. 6f). These observations suggest that auxin signaling is dynamic during style development and is probably key to determining the ultimate length of the mature style.

New Phytologist

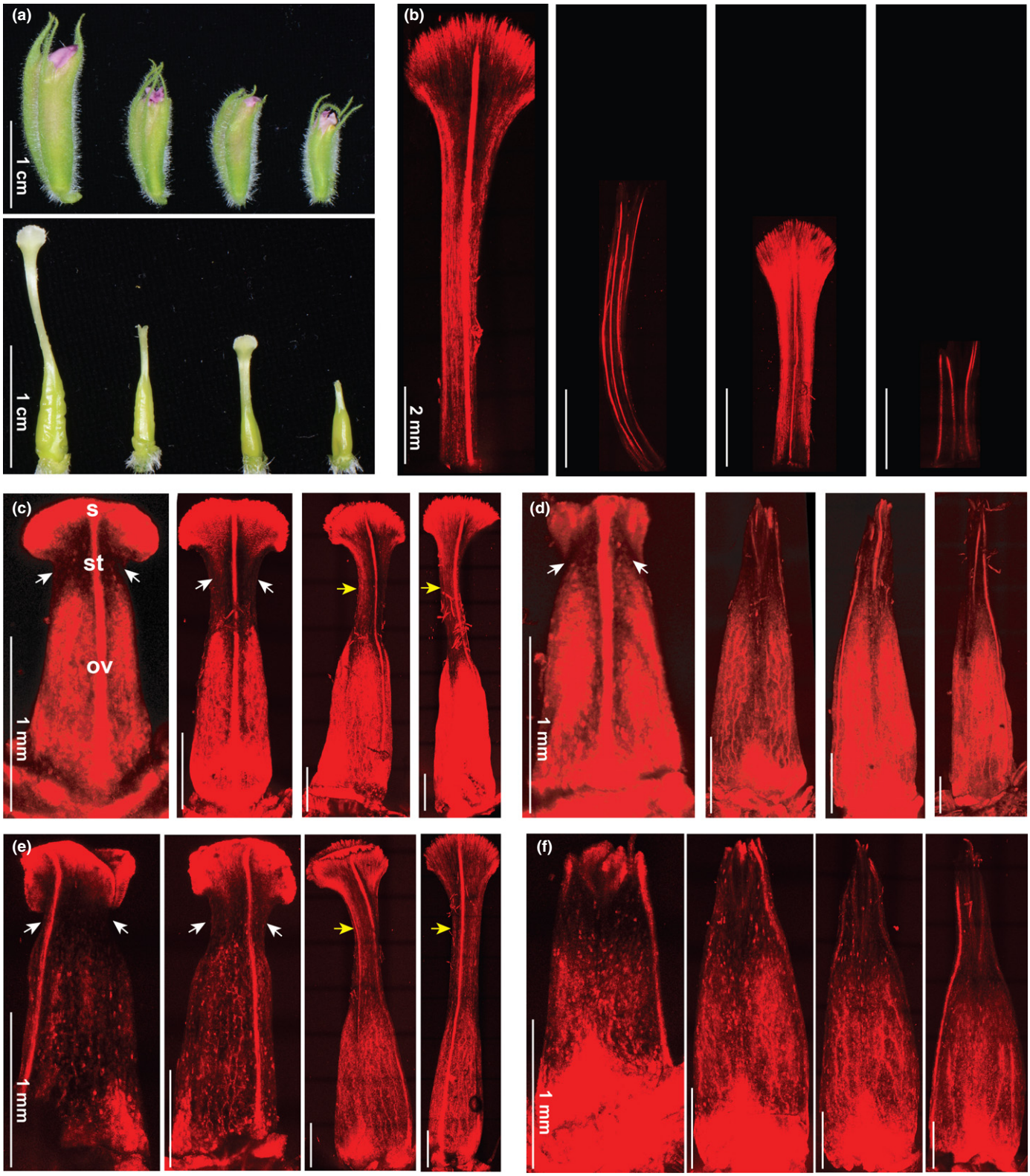

Fig. 6 Patterns of auxin response. (a) Whole floral buds (upper) and pistils (lower) at the 15 mm stage (wild-type, 4 d before anthesis) or equivalent developmental stages of various mutant and transgenic lines (from left to right: wild-type LF10, *mlsgs3-1*, *MlYAB* RNAi, *sgs3 yab* line). (b) Auxin response patterns of the excised styles at the 15 mm stage; genotypes are shown in the same order as in (a). (c) Wild-type pistils at 2, 5, 8 and 10 mm stages (left to right). The white arrows point to the auxin response minimum right below the stigma. The yellow arrows point to the redistributed DR5 signal that correlates with style elongation. s, stigma; st, style; ov, ovary. (d–f) Pistils of *mlsgs3-1* (d), *MlYAB* RNAi (e), and the *sgs3 yab* line (f) at corresponding developmental stages to those shown in (c). Bars: (a) 1 cm; (b) 2 mm; (c–f) 1 mm.

NPA treatment reduces style length in the wild-type

If auxin signaling indeed plays an important role in regulating style elongation, exogenous application of the polar auxin transport inhibitor NPA during the early stages of pistil development may interfere with style elongation. To test this hypothesis, we first attempted to microsurgically apply 100 μM NPA dissolved in lanoline to the pistils of the wild-type flower buds that are < 5 mm long (*c.* 100 flower buds treated). However, this treatment resulted in complete developmental arrest of the flower buds. We then used a 'spray/vacuum infiltration' approach (Nemhauser *et al.*, 2000) to treat the lateral shoot apices, including all flower buds smaller than 5 mm on each lateral shoot. For the mock treatment (distilled water with 0.1% Silwet L-77 and 0.1% DMSO), the first three to four pairs of flower buds (2–5 mm in size) were aborted as a result of the physical damage exerted by the vacuum infiltration. The smaller buds were not impacted by the vacuum infiltration and started to flower about 15 d post-treatment (DPT), and these flowers were indistinguishable from the wild-type flowers.

The NPA treatment caused a delay in flowering and the NPA-treated plants did not start flowering until 25 DPT. About 50% of the flowers that opened between 26 and 30 DPT displayed smaller corollas and shorter styles with otherwise normal flower morphology (Fig. 7a–c; Table S4). Between 30 and 43 DPT, a large number of flowers showed not only shorter styles, but also severely disrupted corolla tubes (Fig. 7d; Table S4). For example, among the 78 flowers measured at 33 DPT, 77% of them had shorter styles and 24% displayed split corollas (Table S4; note that the 77% include flowers with both normal and disrupted corolla tubes). Between 43 and 51 DPT, most flowers that opened during this period were normal, but 7% (15/203) showed symmetry phenotypes (Fig. 7e–h) that closely resemble the *cycloidea* mutant in *Antirrhinum* (snapdragon) (Luo *et al.*, 1996). Curiously, these flowers also phenocopy snapdragon flowers resulting from application of the auxin indoleacetic acid (IAA) to the floral apex before floral organ initiation (Bergbusch, 1999). As both NPA and IAA treatments can switch flowers from bilateral to radial symmetry, we suggest that perhaps it is not the absolute auxin concentration, but rather a dorsoventral asymmetric distribution of auxin signaling, that is required for the patterning of bilaterally symmetric flowers. After 51 DPT, no abnormal flowers were observed. Taken together, our results from the NPA treatment suggest that depending on the floral bud stage when treated with NPA, inhibition of polar auxin transport can impede style and other floral organ elongation, disrupt corolla tube formation (Ding *et al.*, 2020), and interfere with the dorsoventral symmetry program.

Discussion

In this study, we have characterized the role of two classes of leaf adaxial–abaxial polarity factors, SGS3 and the YABBY transcription factors, in the regulation of style elongation in the monkeyflower species *Mimulus lewisii*. Loss of *SGS3* function led to reduced style length via limiting cell division, and RNAi-mediated knockdown of *YABBY* genes resulted in shorter styles by decreasing both cell division and cell elongation. The *sgs3 yab* line showed even more severe reduction of style length and marked alteration in auxin response patterns compared with the wild-type, suggesting a critical role for auxin signaling in style elongation. Given the extensive pleiostropic effects of the *mlsgs3-1* mutation or *MlYAB* RNAi knockdown in both floral and vegetative tissues (Figs 4, S4), it is quite unlikely that these genes contribute directly to natural style length variation between species. However, in order to make clear predictions about which genes in a genetic network are likely to be preferentially selected by evolution to generate phenotypic variation in nature, we need first know most, if not all, of the components of the genetic network underlying the phenotype of interest (Stern, 2011). *SGS3* and the *YABBY* genes can serve as a valuable starting point to identify other components of the genetic network that controls style elongation, especially their downstream genes with less pleiotropic effects and more restricted spatial expression patterns (e.g. style-specific).

A surprising finding from our study is the auxin response minimum right below the stigma in the early-stage pistil of the wild-type *M. lewisii* (Fig. 6c). This auxin response minimum marks a region with attenuated growth during early developmental stages relative to the stigma and the ovary, which differentiates into the style. Despite intensive work on the spatiotemporal pattern of auxin response during pistil development in Arabidopsis (Aloni *et al.*, 2006; Girin *et al.*, 2011; Larsson *et al.*, 2014; Moubayidin & Østergaard, 2014; reviewed in Simonini & Østergaard, 2019), such an auxin response minimum between the stigma and the ovary has not been described. In addition, we observed strong DR5 signals in the *M. lewisii* ovary across all sampled developmental stages, which is in stark contrast to that in the Arabidopsis ovary (Simonini & Østergaard, 2019). The significance of this difference between the two species is currently unclear. On the other hand, the correlation between DR5 signal at the apex of the pistil and stigma formation seems to be a conserved feature between *Mimulus* and Arabidopsis. In the wild-type *M. lewisii*, DR5 signals are strong and continuous along the rim of the pistil apex from the 0.4 mm (corolla diameter) stage onwards (Fig. 6c; also see fig. 6 in Ding *et al.*, 2020 for earlier developmental stages). The same pattern was observed in *MlYAB* RNAi, which shows two normal, flared stigma lobes (Fig. 6e), while the weak and fragmentary DR5 signals at the pistil apex of *mlsgs3-1* or *sgs3 yab* correlate with the malformation of stigma lobes (Fig. 6d,f). In Arabidopsis, a similar 'auxin ring' at the pistil apex has been observed from stage 9 onwards (Girin *et al.*, 2011; Larsson *et al.*, 2014) and was shown to be essential for the formation of the radially symmetric stigmatic surface (Moubayidin & Østergaard, 2014).

Intriguingly, following style differentiation, the auxin response increases in the style (yellow arrows in Fig. 6c), which is correlated with style elongation. This observation suggests that after style differentiation is completed, auxin is redistributed to the style region to promote cell division and elongation. The duration and strength of auxin signaling in the style may determine the ultimate length of the style in the mature flower. The results of our NPA treatment are consistent with this inference (Fig. 7). Although

New Phytologist

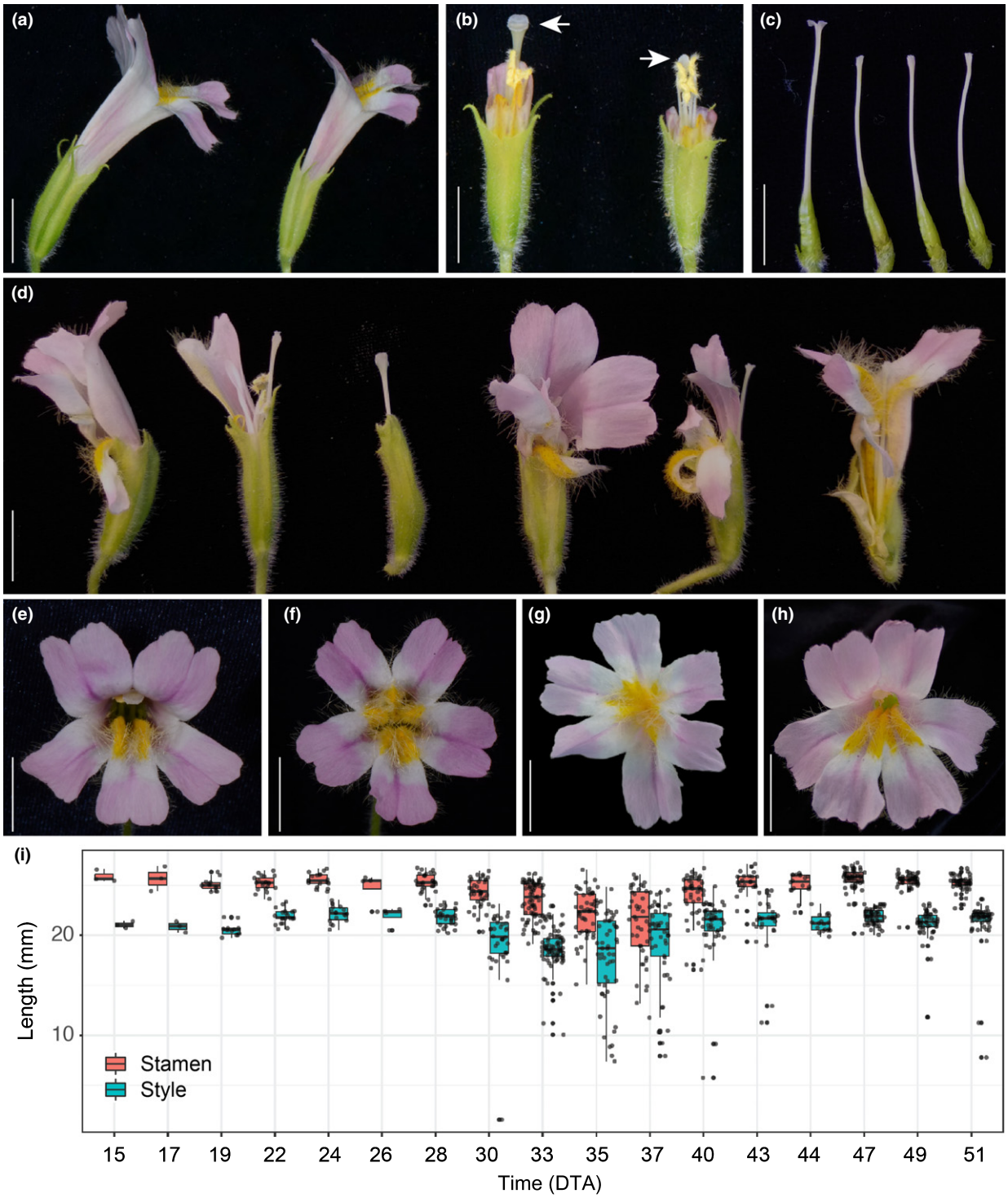

Fig. 7 Phenotypes of N-1-naphthylphthalamic acid (NPA)-treated *Mimulus lewisii* flowers. (a) Side view of a mock-treated (left) and an NPA-treated (right) flower that opened between 26 and 30 d post-treatment (DPT). (b) Side view of the same flowers shown in (a), with petals removed to show the stamens and styles. White arrows point to the stigmas. (c) Pistils of a mock-treated flower (left) and three additional, representative flowers (right) that opened between 26 and 30 DPT. (d) NPA-treated flowers that opened between 30 and 43 DPT showed a range of phenotypes in petal fusion (i.e. corolla tube formation). (e–h) Front view of a mock-treated flower (e) and three NPA-treated flowers (f–h) that opened between 43 and 51 DPT with full or partial conversion from bilateral symmetry to radial symmetry. (i) Measurements of stamen and style length. The NPA-treated plants did not start flowering until 25 d DPT. The data from 15 to 24 DPT are measurements on the mock-treated plants, and data from 26 to 51 DPT are measurements on the NPA-treated plants. Horizontal lines in (i) divide the *y*-axis every 5 mm. The upper whisker is the maximum value of the data that is within 1.5× the interquartile range over the 75th percentile. The lower whisker is the minimum value of the data that is within 1.5× the interquartile range under the 25th percentile. Outlier values are considered any values over 1.5× the interquartile range over the 75th percentile or any values under 1.5× the interquartile range under the 25th percentile. Bars, 10 mm.

auxin has been long recognized as a major player in regional tissue specification during pistil morphogenesis (Nemhauser *et al.*, 2000; Staldal & Sundberg, 2009; Hawkins & Liu, 2014; Larsson *et al.*, 2014; Simonini & Østergaard, 2019), its role in style elongation has been rarely discussed in the literature. One notable exception is a study (Li *et al.*, 2018) in *Nicotiana attenuata* (coyote tobacco), which also produces flowers with a well-differentiated and elongated style. Li *et al.* (2018) not only showed that decreased auxin concentration directly caused stunted styles, but also demonstrated that even the short-style phenotype in jasmonate (JA) signaling-deficient *N. attenuata* genotypes (Stitz *et al.*, 2014) are ultimately caused by reduced auxin signaling. It would be of great interest to image similar auxin-responsive reporters in *Mimulus* and *Nicotiana* styles, to test whether these two distantly related plant lineages have conserved spatiotemporal patterns of auxin signaling during style development.

Three observations suggest that *SGS3* and the *YABBY* genes act synergistically in the regulation of style elongation in *Mimulus*, potentially through the ARF3-KANADI regulatory complex: the *sgs3 yab* line has markedly shorter style than both *mlsgs3-1* and *MlYAB* RNAi (Fig. 4a,c); the changes in auxin response patterns in the *sgs3 yab* pistil show features of both the *mlsgs3-1* single mutant (i.e. DR5 signal is restricted to a few parallel veins) and *MlYAB* RNAi (i.e. weaker DR5 signal in the ovary) (Fig. 4d–f); and *ARF3/4* are upregulated to a greater extent in *sgs3 yab* than *mlsgs3-1* or *MlYAB* RNAi and the *KANADI* genes are significantly upregulated in the *sgs3 yab* style but show no change in the style of either *mlsgs3-1* or *MlYAB* RNAi. Interestingly, a petunia mutant, *choripetala suzanne* (*chsu*), is very similar to the *M. lewisii ago7* and *sgs3* mutants. It also produces flowers with unfused corollas and shorter styles and has increased *ARF3/4* expression (Vandenbussche *et al.*, 2009). Furthermore, when crossed with another leaf polarity mutant *maewest* (*maw*, the petunia ortholog of Arabidopsis *WOX1*), the *chsu maw* double mutant shows synergistic upregulation of both the *ARF3/4* and *KANADI* genes. Although the molecular identity of *CHSU* is still unknown, these parallel changes in leaf polarity gene expression between *Mimulus* and petunia suggest that the genetic control of pistil development and style elongation is conserved across the asterid clade, where both *Mimulus* and petunia belong.

Carpels, like other floral organs, are widely considered as modified leaves (Scutt *et al.*, 2006), and the leaf polarity network is believed to have played a critical role in the formation of carpels in the most recent common ancestor of angiosperms (Ferrandiz *et al.*, 2010; Hawkins & Liu, 2014). However, whether the leaf polarity network has been coopted to regulate style elongation as well is not immediately obvious, as the first carpel at the origin of angiosperms is most probably ascidiate and lacks a style (Endress & Doyle, 2015). Our results demonstrate that both adaxial and abaxial factors of the leaf polarity network are involved in style elongation, and therefore it seems plausible that the whole leaf polarity network has been coopted to regulate style elongation. It should be noted that this cooption for style elongation is probably independent of the cooption that enabled the origin of carpels, and happened later during angiosperm evolution, that is, after the divergence from the basal ANA (*Amborella*, Nymphaeales and Austrobaileyales) grade, which retain many of the ancestral features of angiosperm carpels and lack an elongated style. Although our results indicate that these leaf polarity regulators affect style length through auxin dynamics, how they exactly regulate the biosynthesis, transport and signaling of auxin in the developing style remains to be elucidated.

While we suggest that auxin signaling plays a central role in style elongation, we should also point out that there are probably complex cross-talks among different hormone signaling pathways. The aforementioned JA regulation of style length in *N. attenuata* (Stitz *et al.*, 2014) was shown to be mediated through auxin signaling (Li *et al.*, 2018). The *CYP734A50* gene that determines the style-length dimorphism in *Primula* encodes a putative brassinosteroid-degrading enzyme, and exogenous brassinosteroid treatment could convert the short style to a long style (Huu *et al.*, 2016). The Arabidopsis homologs of STYLE2.1, which controls style length variation between domesticated tomatoes and their wild relatives, were shown to regulate cell elongation downstream of brassinosteroid and gibberellin signaling (Bai *et al.*, 2012; Ikeda *et al.*, 2012). Sorting out how these hormone signaling pathways cross-talk with each other will be important in obtaining a deeper understanding of the developmental genetic control of style elongation.

Acknowledgements

We thank Clinton Morse, Matt Opel and Adam Histen for extraordinary plant care in the UConn EEB Research Greenhouses. We are grateful to Dr Pamela Diggle for sharing her microscope and providing technical assistance for cell measurements. We thank three anonymous reviewers for their constructive criticism. This work was supported by an NSF grant (IOS-1755373) to Y-WY.

Author contributions

BD and Y-WY planned and designed the research. BD and JL performed most of the phenotypic characterization and functional experiments. VG and QL assisted with SEM and confocal imaging. XS contributed to the transgenic experiment. BD and Y-WY wrote the manuscript with input from all authors. BD and JL contributed equally to this work.

ORCID

Baoqing Ding https://orcid.org/0000-0001-7183-9653
Vandana Gurung https://orcid.org/0000-0001-5128-876X
Jingjian Li https://orcid.org/0000-0002-0547-0736
Qiaoshan Lin https://orcid.org/0000-0001-7851-6048
Xuemei Sun https://orcid.org/0000-0002-8811-1244
Yao-Wu Yuan https://orcid.org/0000-0003-1376-0028

Data availability

The data that support the findings of this study are available in the supplementary material of this article.

References

Abramoff MD, Magalhães PJ, Ram SJ. 2004. Image processing with ImageJ. *Biophotonics International* **11**: 36–42.

Allen E, Xie Z, Gustafson AM, Carrington JC. 2005. microRNA-directed phasing during trans-acting siRNA biogenesis in plants. *Cell* **121**: 207–221.

Aloni R, Aloni E, Langhans M, Ullrich CI. 2006. Role of auxin in regulating *Arabidopsis* flower development. *Planta* **223**: 315–328.

Arunkumar R, Wang W, Wright SI, Barrett SCH. 2017. The genetic architecture of tristyly and its breakdown to self-fertilization. *Molecular Ecology* **26**: 752–765.

Axtell MJ, Jan C, Rajagopalan R, Bartel DP. 2006. A two-hit trigger for siRNA biogenesis in plants. *Cell* **127**: 565–577.

Bai MY, Fan M, Oh E, Wang ZY. 2012. A triple helix-loop-helix/basic helix-loop-helix cascade controls cell elongation downstream of multiple hormonal and environmental signaling pathways in *Arabidopsis*. *Plant Cell* **24**: 4917–4929.

Barrett SC. 2002. The evolution of plant sexual diversity. *Nature Reviews Genetics* **3**: 274–284.

Barrett SC. 2010. Understanding plant reproductive diversity. *Philosophical Transactions of the Royal Society B: Biological Sciences* **365**: 99–109.

Barrett SCH. 2019. 'A most complex marriage arrangement': recent advances on heterostyly and unresolved questions. *New Phytologist* **224**: 1051–1067.

Barrett SCH, Jesson LK, Baker AM. 2000. The evolution and function of stylar polymorphisms in flowering plants. *Annals of Botany* **85**(Suppl: A): 253–265.

Bergbusch VL. 1999. A Note on the manipulation of flower symmetry in *Antirrhinum majus*. *Annals of Botany* **83**: 483–488.

Bernacchi D, Tanksley SD. 1997. An interspecific backcross of *Lycopersicon esculentum* x *L. hirsutum*: linkage analysis and a QTL study of sexual compatibility factors and floral traits. *Genetics* **147**: 861–877.

Bowman JL. 2000. The YABBY gene family and abaxial cell fate. *Current Opinion in Plant Biology* **3**: 17–22.

Bradshaw HD, Wilbert SM, Otto KG, Schemske DW. 1995. Genetic-mapping of floral traits associated with reproductive isolation in monkeyflowers (*Mimulus*). *Nature* **376**: 762–765.

Brandt R, Salla-Martret M, Bou-Torrent J, Musielak T, Stahl M, Lanz C, Ott F, Schmid M, Greb T, Schwarz M *et al.* 2012. Genome-wide binding-site analysis of REVOLUTA reveals a link between leaf patterning and light-mediated growth responses. *The Plant Journal* **72**: 31–42.

Chen KY, Cong B, Wing R, Vrebalov J, Tanksley SD. 2007. Changes in regulation of a transcription factor lead to autogamy in cultivated tomatoes. *Science* **318**: 643–645.

Chen KY, Tanksley SD. 2004. High-resolution mapping and functional analysis of *se2.1*: a major stigma exsertion quantitative trait locus associated with the evolution from allogamy to autogamy in the genus *Lycopersicon*. *Genetics* **168**: 1563–1573.

Chitwood DH, Nogueira FT, Howell MD, Montgomery TA, Carrington JC, Timmermans MC. 2009. Pattern formation via small RNA mobility. *Genes & Development* **23**: 549–554.

Darwin C. 1877. *The different forms of flowers on plants of the same species*. New York, NY, USA: D. Appleton & Co.

Ding B, Mou F, Sun W, Chen S, Peng F, Bradshaw HD, Yuan Y-W. 2017. A dominant-negative actin mutation alters corolla tube width and pollinator visitation in *Mimulus lewisii*. *New Phytologist* **213**: 1936–1944.

Ding B, Xia R, Lin Q, Gurung V, Sagawa JM, Stanley LE, Strobel M, Diggle PK, Meyers BC, Yuan Y-W. 2020. Developmental genetics of corolla tube formation: role of the tasiRNA-*ARF* pathway and a conceptual model. *Plant Cell* **32**: 3452–3468.

Douglas RN, Wiley D, Sarkar A, Springer N, Timmermans MCP, Scanlon MJ. 2010. *ragged seedling2* encodes an *ARGONAUTE7*-Like protein required for mediolateral expansion, but not dorsiventrality, of maize leaves. *Plant Cell* **22**: 1441–1451.

Dulberger R. 1992. Floral polymorphisms and their functional significance in the heterostylous syndrome. In: Barrett SCH ed. *Evolution and function of heterostyly*. Berlin/Heidelberg, Germany: Springer, 41–84.

Endress PK, Doyle JA. 2015. Ancestral traits and specializations in the flowers of the basal grade of living angiosperms. *Taxon* **64**: 1093–1116.

Eshed Y, Baum SF, Bowman JL. 1999. Distinct mechanisms promote polarity establishment in carpels of *Arabidopsis*. *Cell* **99**: 199–209.

Fahlgren N, Montgomery TA, Howell MD, Allen E, Dvorak SK, Alexander AL, Carrington JC. 2006. Regulation of AUXIN RESPONSE FACTOR3 by TAS3 ta-siRNA affects developmental timing and patterning in *Arabidopsis*. *Current Biology* **16**: 939–944.

Ferrandiz C, Fourquin C, Prunet N, Scutt CP, Sundberg E, Trehin C, Vialette-Guiraud AC. 2010. Carpel development. *Advances in Botanical Research* **55**: 1–73.

Fishman L, Beardsley PM, Stathos A, Williams CF, Hill JP. 2015. The genetic architecture of traits associated with the evolution of self-pollination in Mimulus. *New Phytologist* **205**: 907–917.

Fishman L, Kelly AJ, Willis JH. 2002. Minor quantitative trait loci underlie floral traits associated with mating system divergence in *Mimulus*. *Evolution* **56**: 2138–2155.

Franks RG, Wang C, Levin JZ, Liu Z. 2002. *SEUSS*, a member of a novel family of plant regulatory proteins, represses floral homeotic gene expression with *LEUNIG*. *Development* **129**: 253–263.

Ganders FR. 1979. The biology of heterostyly. *New Zealand Journal of Botany* **17**: 607–635.

Garcia D, Collier SA, Byrne ME, Martienssen RA. 2006. Specification of leaf polarity in *Arabidopsis* via the trans-acting siRNA pathway. *Current Biology* **16**: 933–938.

Georgiady MS, Whitkus RW, Lord EM. 2002. Genetic analysis of traits distinguishing outcrossing and self-pollinating forms of currant tomato, *Lycopersicon pimpinellifolium* (Jusl.) Mill. *Genetics* **161**: 333–344.

Girin T, Paicu T, Stephenson P, Fuentes S, Körner E, O'Brien M, Sorefan K, Wood TA, Balanzá V, Ferrándiz C *et al.* 2011. *INDEHISCENT* and *SPATULA* interact to specify carpel and valve margin tissue and thus promote seed dispersal in *Arabidopsis*. *Plant Cell* **23**: 3641–3653.

Golz JF, Roccaro M, Kuzoff R, Hudson A. 2004. *GRAMINIFOLIA* promotes growth and polarity of *Antirrhinum* leaves. *Development* **131**: 3661–3670.

Goodwillie C, Ritland C, Ritland K. 2006. The genetic basis of floral traits associated with mating system evolution in *Leptosiphon* (Polemoniaceae): an analysis of quantitative trait loci. *Evolution* **60**: 491–504.

Han Y, Burnette JM III, Wessler SR. 2009. TARGeT: a web-based pipeline for retrieving and characterizing gene and transposable element families from genomic sequences. *Nucleic Acids Research* **37**: e78.

Hawkins C, Liu Z. 2014. A model for an early role of auxin in *Arabidopsis* gynoecium morphogenesis. *Frontiers in Plant Science* **5**: 327.

Hazle T. 2001. *Ontogenetic evolution and speciation in* Mimulus cardinalis *and* M. lewisii (*Lamiales*). MS thesis, University of Guelph, Guelph, Ontario, Canada.

Hazle T, Canne-Hilliker J. 2005. Floral ontogeny and allometry of *Mimulus Cardinalis:* Interpopulational variation and traits of the hummingbird-pollination syndrome. *International Journal of Plant Sciences* **166**: 61–83.

Heisler MG, Atkinson A, Bylstra YH, Walsh R, Smyth DR. 2001. *SPATULA*, a gene that controls development of carpel margin tissues in *Arabidopsis*, encodes a bHLH protein. *Development* **128**: 1089–1098.

Hermann K, Klahre U, Venail J, Brandenburg A, Kuhlemeier C. 2015. The genetics of reproductive organ morphology in two *Petunia* species with contrasting pollination syndromes. *Planta* **241**: 1241–1254.

Huang T, Harrar Y, Lin C, Reinhart B, Newell NR, Talavera-Rauh F, Hokin SA, Barton MK, Kerstetter RA. 2014. Arabidopsis KANADI1 acts as a transcriptional repressor by interacting with a specific cis-element and regulates auxin biosynthesis, transport, and signaling in opposition to HD-ZIPIII factors. *Plant Cell* **26**: 246–262.

Hunter C, Willmann MR, Wu G, Yoshikawa M, de la Luz G-N, Poethig SR. 2006. Trans-acting siRNA-mediated repression of *ETTIN* and *ARF4* regulates heteroblasty in *Arabidopsis*. *Development* **133**: 2973–2981.

Huu CN, Kappel C, Keller B, Sicard A, Takebayashi Y, Breuninger H, Nowak MD, Bäurle I, Himmelbach A, Burkart M *et al.* 2016. Presence versus absence of *CYP734A50* underlies the style-length dimorphism in *primroses*. *eLife* **5**: e17956.

Ikeda M, Fujiwara S, Mitsuda N, Ohme-Takagi M. 2012. A triantagonistic basic helix-loop-helix system regulates cell elongation in *Arabidopsis*. *Plant Cell* **24**: 4483–4497.

Iwasaki M, Takahashi H, Iwakawa H, Nakagawa A, Ishikawa T, Tanaka H, Matsumura Y, Pekker I, Eshed Y, Vial-Pradel S. 2013. Dual regulation of *ETTIN* (*ARF3*) gene expression by AS1-AS2, which maintains the DNA methylation level, is involved in stabilization of leaf adaxial-abaxial partitioning in Arabidopsis. *Development* **140**: 1958–1969.

Kelley DR, Arreola A, Gallagher TL, Gasser CS. 2012. ETTIN (ARF3) physically interacts with KANADI proteins to form a functional complex essential for integument development and polarity determination in Arabidopsis. *Development* **139**: 1105–1109.

Kerschen A, Napoli CA, Jorgensen RA, Müller AE. 2004. Effectiveness of RNA interference in transgenic plants. *FEBS Letters* **566**: 223–228.

Kostyun JL, Gibson MJS, King CM, Moyle LC. 2019. A simple genetic architecture and low constraint allow rapid floral evolution in a diverse and recently radiating plant genus. *New Phytologist* **223**: 1009–1022.

Kuhlemeier C, Timmermans MCP. 2016. The Sussex signal: insights into leaf dorsiventrality. *Development* **143**: 3230–3237.

Kuusk S, Sohlberg JJ, Long JA, Fridborg I, Sundberg E. 2002. *STY1*and *STY2* promote the formation of apical tissues during *Arabidopsis* gynoecium development. *Development* **129**: 4707–4717.

Labonne JDJ, Shore JS. 2011. Positional cloning of the s haplotype determining the floral and incompatibility phenotype of the long-styled morph of distylous *Turnera subulata*. *Molecular Genetics and Genomics* **285**: 101–111.

Larsson A. 2014. AliView: a fast and lightweight alignment viewer and editor for large datasets. *Bioinformatics* **30**: 3276–3278.

Larsson E, Roberts CJ, Claes AR, Franks RG, Sundberg E. 2014. Polar auxin transport is essential for medial versus lateral tissue specification and vascular-mediated valve outgrowth in *Arabidopsis* gynoecia. *Plant Physiology* **166**: 1998–2012.

Li J, Schuman MC, Halitschke R, Li X, Guo H, Grabe V, Hammer A, Baldwin IT. 2018. The decoration of specialized metabolites influences stylar development. *eLife* **7**: e38611.

Liljegren SJ, Roeder AHK, Kempin SA, Gremski K, Østergaard L, Guimil S, Reyes DK, Yanofsky MF. 2004. Control of fruit patterning in *Arabidopsis* by *INDEHISCENT*. *Cell* **116**: 843–853.

Luo D, Carpenter R, Vincent C, Copsey L, Coen E. 1996. Origin of floral asymmetry in *Antirrhinum*. *Nature* **383**: 794–799.

Merelo P, Xie Y, Brand L, Ott F, Weigel D, Bowman JL, Heisler MG, Wenkel S. 2013. Genome-wide identification of KANADI1 target genes. *PLoS ONE* **8**: e77341.

Moubayidin L, Østergaard L. 2014. Dynamic control of auxin distribution imposes a bilateral-to-radial symmetry switch during gynoecium development. *Current Biology* **24**: 2743–2748.

Nagasaki H, Itoh J-I, Hayashi K, Hibara K-I, Satoh-Nagasawa N, Nosaka M, Mukouhata M, Ashikari M, Kitano H, Matsuoka M *et al.* 2007. The small interfering RNA production pathway is required for shoot meristem initiation in rice. *Proceedings of the National Academy of Sciences, USA* **104**: 14867–14871.

Nakata M, Okada K. 2013. The leaf adaxial-abaxial boundary and lamina growth. *Plants* **2**: 174–202.

Nemhauser JL, Feldman LJ, Zambryski PC. 2000. Auxin and *ETTIN* in *Arabidopsis* gynoecium morphogenesis. *Development* **127**: 3877–3888.

Nogueira FT, Madi S, Chitwood DH, Juarez MT, Timmermans MC. 2007. Two small regulatory RNAs establish opposing fates of a developmental axis. *Genes and Development* **21**: 750–755.

Pekker I, Alvarez JP, Eshed Y. 2005. Auxin response factors mediate Arabidopsis organ asymmetry via modulation of KANADI activity. *Plant Cell* **17**: 2899–2910.

Pfluger J, Zambryski P. 2004. The role of *SEUSS* in auxin response and floral organ patterning. *Development* **131**: 4697–4707.

R Development Core Team. 2021. R: A language and environment for statistical computing, v.4.0.4. Vienna, Austria: R Foundation for Statistical Computing. [WWW document] URL http://www.R-project.org.

Renner SS. 2014. The relative and absolute frequencies of angiosperm sexual systems: dioecy, monoecy, gynodioecy, and an updated online database. *American Journal of Botany* **101**: 1588–1596.

Roeder AHK, Ferrándiz C, Yanofsky MF. 2003. The role of the *REPLUMLESS* homeodomain protein in patterning the *Arabidopsis* fruit. *Current Biology* **13**: 1630–1635.

Sagawa JM, Stanley LE, LaFountain AM, Frank HA, Liu C, Yuan Y-W. 2016. An R2R3-MYB transcription factor regulates carotenoid pigmentation in *Mimulus lewisii* flowers. *New Phytologist* **209**: 1049–1057.

Sarojam R, Sappl PG, Goldshmidt A, Efroni I, Floyd SK, Eshed Y, Bowman JL. 2010. Differentiating *Arabidopsis* shoots from leaves by combined *YABBY* activities. *Plant Cell* **22**: 2113–2130.

Sawa S, Watanabe K, Goto K, Liu YG, Shibata D, Kanaya E, Morita EH, Okada K. 1999. *FILAMENTOUS FLOWER*, a meristem and organ identity gene of *Arabidopsis*, encodes a protein with a zinc finger and HMG-related domains. *Genes and Development* **13**: 1079–1088.

Scutt CP, Vinauger-Douard M, Fourquin C, Finet C, Dumas C. 2006. An evolutionary perspective on the regulation of carpel development. *Journal of Experimental Botany* **57**: 2143–2152.

Sessions A, Nemhauser JL, McColl A, Roe JL, Feldmann KA, Zambryski PC. 1997. *ETTIN* patterns the *Arabidopsis* floral meristem and reproductive organs. *Development* **124**: 4481–4491.

Simonini S, Deb J, Moubayidin L, Stephenson P, Valluru M, Freire-Rios A, Sorefan K, Weijers D, Friml J, Ostergaard L. 2016. A noncanonical auxin-sensing mechanism is required for organ morphogenesis in *Arabidopsis*. *Genes and Development* **30**: 2286–2296.

Simonini S, Østergaard L. 2019. Chapter Thirteen - Female reproductive organ formation: A multitasking endeavor. In: Grossniklaus U, ed. *Current topics in developmental biology*. Cambridge, MA, USA: Academic Press, 337–371.

Simonini S, Stephenson P, Østergaard L. 2018. A molecular framework controlling style morphology in *Brassicaceae*. *Development* **145**: dev158105.

Staldal V, Sundberg E. 2009. The role of auxin in style development and apical-basal patterning of the *Arabidopsis thaliana* gynoecium. *Plant Signaling & Behavior* **4**: 83–85.

Stanley LE, Ding B, Sun W, Mou F, Hill C, Chen S, Yuan YW. 2020. A tetratricopeptide repeat protein regulates carotenoid biosynthesis and chromoplast development in Monkeyflowers (*Mimulus*). *Plant Cell* **32**: 1536–1555.

Stern DL. 2011. *Evolution, development, and the predictable genome*. Greenwood Village, CO, USA: Roberts & Co.

Stitz M, Hartl M, Baldwin IT, Gaquerel E. 2014. Jasmonoyl-L-isoleucine coordinates metabolic networks required for anthesis and floral attractant emission in wild tobacco (*Nicotiana attenuata*). *Plant Cell* **26**: 3964–3983.

Swofford D. 2002. *PAUP* Phylogenetic analysis using parsimony (* and other methods) v. 4.0 b10*. Sunderland, MA, USA: Sinauer Associates.

Tsukaya H. 2013. Leaf development. *The Arabidopsis Book* **11**: e0163.

Ushijima K, Ikeda K, Nakano R, Matsubara M, Tsuda Y, Kubo Y. 2015. Genetic control of floral morph and petal pigmentation in *Linum grandiflorum* Desf., a Heterostylous Flax. *Horticulture Journal* **84**: 261–268.

Vandenbussche M, Horstman A, Zethof J, Koes R, Rijpkema AS, Gerats T. 2009. Differential recruitment of WOX transcription factors for lateral development and organ fusion in *Petunia* and *Arabidopsis*. *Plant Cell* **21**: 2269–2283.

Venglat SP, Dumonceaux T, Rozwadowski K, Parnell L, Babic V, Keller W, Martienssen R, Selvaraj G, Datla R. 2002. The homeobox gene *BREVIPEDICELLUS* is a key regulator of inflorescence architecture in *Arabidopsis*. *Proceedings of the National Academy of Sciences, USA* **99**: 4730–4735.

Villanueva JM, Broadhvest J, Hauser BA, Meister RJ, Schneitz K, Gasser CS. 1999. *INNER NO OUTER* regulates abaxial- adaxial patterning in *Arabidopsis* ovules. *Genes and Development* **13**: 3160–3169.

Waites R, Hudson A. 1995. *Phantastica*: a gene required for dorsoventrality of leaves in *Antirrhinum majus*. *Development* **121**: 2143–2154.

Wessinger CA, Hileman LC, Rausher MD. 2014. Identification of major quantitative trait loci underlying floral pollination syndrome divergence in *Penstemon*. *Philosophical Transactions of the Royal Society of London. Series B: Biological Sciences* **369**: 20130349.

Wu G, Lin W-C, Huang T, Poethig RS, Springer PS, Kerstetter RA. 2008. KANADI1 regulates adaxial-abaxial polarity in Arabidopsis by directly repressing the transcription of ASYMMETRIC LEAVES2. *Proceedings of the National Academy of Sciences, USA* **105**: 16392–16397.

Yan J, Cai X, Luo J, Sato S, Jiang Q, Yang J, Cao X, Hu X, Tabata S, Gresshoff PM *et al.* 2010. The *REDUCED LEAFLET* genes encode key components of the trans-acting small interfering RNA pathway and regulate compound leaf and flower development in *Lotus japonicus*. *Plant Physiology* **152**: 797–807.

Yarahmadov T, Robinson S, Hanemian M, Pulver V, Kuhlemeier C. 2020. Identification of transcription factors controlling floral morphology in wild *Petunia* species with contrasting pollination syndromes. *The Plant Journal* **104**: 289–301.

Yasui Y, Hirakawa H, Ueno M, Matsui K, Katsube-Tanaka T, Yang SJ, Aii J, Sato S, Mori M. 2016. Assembly of the draft genome of buckwheat and its applications in identifying agronomically useful genes. *DNA Research* **23**: 215–224.

Yifhar T, Pekker I, Peled D, Friedlander G, Pistunov A, Sabban M, Wachsman G, Alvarez JP, Amsellem Z, Eshed Y. 2012. Failure of the tomato trans-acting short interfering RNA program to regulate *AUXIN RESPONSE FACTOR3* and *ARF4* underlies the Wiry Leaf Syndrome. *Plant Cell* **24**: 3575–3589.

Yuan Y-W, Sagawa JM, Di Stilio VS, Bradshaw HD. 2013a. Bulk segregant analysis of an induced floral mutant identifies a *MIXTA*-like *R2R3 MYB* controlling nectar guide formation in *Mimulus lewisii*. *Genetics* **194**: 523–528.

Yuan Y-W, Sagawa JM, Frost L, Vela JP, Bradshaw HD. 2014. Transcriptional control of floral anthocyanin pigmentation in monkeyflowers (*Mimulus*). *New Phytologist* **204**: 1013–1027.

Yuan Y-W, Sagawa JM, Young RC, Christensen BJ, Bradshaw HD. 2013b. Genetic dissection of a major anthocyanin QTL contributing to pollinator-mediated reproductive isolation between sister species of *Mimulus*. *Genetics* **194**: 255–263.

Zhou C, Han L, Fu C, Wen J, Cheng X, Nakashima J, Ma J, Tang Y, Tan Y, Tadege M *et al.* 2013. The trans-acting short interfering RNA3 pathway and *NO APICAL MERISTEM* antagonistically regulate leaf margin development and lateral organ separation, as revealed by analysis of an *argonaute7/lobed leaflet1* mutant in *Medicago truncatula*. *Plant Cell* **25**: 4845–4862.

Supporting Information

Additional Supporting Information may be found online in the Supporting Information section at the end of the article.

Fig. S1 Amino acid alignment of the YABBY family transcription factors.

Fig. S2 Exemplar panoramic cell-profile images of the excised full-length styles.

Fig. S3 Phenotypes of the wild-type and three *MlYAB* RNAi transgenic lines.

Fig. S4 Phenotypes of the wild-type, *mlsgs3-1*, *MlYAB* RNAi and the *sgs3 yab* line.

Table S1 Primers used in this study.

Table S2 Measurements of the lengths of the long stamen, pistil, style and ovary.

Table S3 Average cell length of every 10 contiguous cells along the styles.

Table S4 Frequency of altered phenotypes among NPA-treated *Mimulus* flowers.

Please note: Wiley Blackwell are not responsible for the content or functionality of any Supporting Information supplied by the authors. Any queries (other than missing material) should be directed to the *New Phytologist* Central Office.